Systematic template extraction from chaotic attractors: II. Genus-one attractors with multiple unimodal folding mechanisms

Martin Rosalie, Christophe Letellier

▶ **To cite this version:**

Martin Rosalie, Christophe Letellier. Systematic template extraction from chaotic attractors: II. Genus-one attractors with multiple unimodal folding mechanisms. Journal of Physics A: Mathematical and Theoretical, 2015, 48 (23), pp.235101. ⟨10.1088/1751-8113/48/23/235101⟩. ⟨hal-01159666⟩

HAL Id: hal-01159666

https://hal.science/hal-01159666v1

Submitted on 10 Aug 2016

HAL is a multi-disciplinary open access archive for the deposit and dissemination of scientific research documents, whether they are published or not. The documents may come from teaching and research institutions in France or abroad, or from public or private research centers.

L'archive ouverte pluridisciplinaire **HAL**, est destinée au dépôt et à la diffusion de documents scientifiques de niveau recherche, publiés ou non, émanant des établissements d'enseignement et de recherche français ou étrangers, des laboratoires publics ou privés.

HAL Authorization

Systematic template extraction from chaotic attractors. II Genus-one attractors with multiple unimodal folding mechanisms

Martin Rosalie & Christophe Letellier

CORIA-UMR 6614 Normandie Université, CNRS-Université et INSA de Rouen, Campus Universitaire du Madrillet, F-76800 Saint-Etienne du Rouvray, France

E-mail: martin.rosalie@coria.fr

Abstract. Asymmetric and symmetric chaotic attractors produced by the simplest jerk equivariant system are topologically characterized. In the case of this system with an inversion symmetry, it is shown that symmetric attractors bounded by genus-one tori are conveniently analyzed using a two-components Poincaré section. Resulting from a merging attractor crisis, these attractors can be easily described as made of two foldings mechanisms (here described as mixers), one for each of the two attractors co-existing before the crisis: symmetric attractors are thus described by a template made of two mixers. We thus developed a procedure for concatenating two mixers (here associated with unimodal maps) into a single one, allowing to describe a reduced template, that is, a template simplified under an isotopy. The so-obtained reduced template is associated with a description of symmetric attractors based on one-component Poincaré section as suggested by the corresponding genus-one bounding torus. It is shown that several reduced templates can be obtained depending on the choice of the retained one-component Poincaré section.

PACS numbers: 05.45.-a

Keywords: Topological characterization, template, linking matrix, genus-1 attractor, unimodal folding mechanism

Submitted to: *J. Phys. A: Math. Gen. 24 November 2014*

1. Introduction

In a recent paper, we proposed a systematic procedure to extract template for genus-one chaotic attractors with a single folding mechanism, that is, for attractor bounded by a genus-one torus [1, 2] and characterized by a unimodal smooth first-return map [3]. The procedure was developed for attractor with a single folding mechanism between two successive intersections with a given Poincaré section. This type of attractors corresponds to the Rössler attractor [4] as well as many other attractors (see [5, 6, 7, 8, 9, 10, 11], for instance). When the system presents an inversion symmetry as encountered in the simplest equivariant jerk system [12], there are some parameter values for which the attractor presents two foldings, thus leading to a trimodal map [13, 14]. Such a case occurs in fact in any system with an order-2 symmetry presenting a merging attractor crisis [13, 15]. It can be also observed in the Lorenz system for large R parameter values [16]. In that cases, the trimodal first-return map which characterizes such attractor can be viewed as the product of two unimodal smooth maps.

According to our previous work [3], any template can be described by a linker made of splitting chart which divides the attractor in branches [17], torsion (local or/and global), permutations and branch insertion where branches are squeezed [17, 18]. For instance, a simple folding as observed in the spiral Rössler attractor [4, 19] is characterized by a simple mixer made of a splitting chart inducing two branches, one having a local negative torsion (a negative half-turn), and one negative permutation between the two branches which are squeezed at a branch line matching, for instance, with the one-component Poincaré section. A mixer is described by a single linking matrix encoding torsion of each branch (diagonal elements) and permutation between branches (off-diagonal elements) [17]; the template of the spiral Rössler attractor is thus described by a simple linking matrix [19].

When an attractor has two foldings (two stretching and squeezing mechanisms) as the symmetric attractor observed in the simplest equivariant jerk system, its topological description must be made by using two branch lines (at which the branches are squeezed), being associated with each of them. In our previous work, only attractors with a single folding, that is, a single mixer were considered. When there are some global torsions, we showed that the linking matrix can be decomposed into a sum of linking matrices, one describing the folding and the others each global torsion for instance [3]: in such a case, we had to consider the addition of linking matrices. When the considered attractor is made of two foldings (two branch lines), the two mixers have to be combined in a multiplicative way for getting a reduced template, that is, a template made of a single mixer as it was done for instance in investigating the Burke and Shaw attractor [13] or as briefly suggested in [20]. In the present work, our aim is to show that the unique 4×4 linking matrix used for describing such a reduced template can be obtained by the product of the two 2×2 linking matrices describing the two mixers: such a multiplicative law will be particularly useful for characaterizing attractors with multiple foldings because it is easier to construct a mixer for each of the folding than one for the reduced template. With such a multiplicative law, the procedure for characterizing an attractor with two foldings would be to get the two mixers (their linking matrices) and then to apply the multiplicative law. In other words, when an attractor has two unimodal foldings, each of them being made of two branches, it can be described with a single mixer (folding) made of four branches which can be viewed as the product of the two two-branch mixers. This multiplicative

law that we will introduce in this paper appears as the required companion to the additive law introduced in our previous work [3] to develop a systematic procedure for extracting templates for attractors with multiple foldings. The present work concerns attractors bounded by genus-one tori.

The subsequent part of this paper is organized as follows. In section 2 we sum up our previous work to describe a template in terms of linker. The system under study, the simplest equivariant jerk system obtained by Malasoma [12], is also introduced. In section 3, we topologically characterized the symmetric attractor combining two foldings and obtained its reduced template using a one-component Poincaré section, that is, without taking into account the inversion symmetry of the system. In section 4, we investigated the symmetric attractor with a two-component Poincaré section that permits to obtain two mixers in which the symmetry of the system is thus explicitly described. The direct template reveals the two mixers corresponding to the two asymmetric attractors that merged via a crisis to form a single symmetric attractor. Section 6 gives some conclusions.

2. Coexisting asymmetric attractors in a simple equivariant system

2.1. The simplest equivariant jerk system

As in the companion of the present paper, we will investigate the chaotic attractor solution to the simplest equivariant jerk system

$$\begin{cases} \dot{x} = y \\ \dot{y} = z \\ \dot{z} = -\alpha z + xy^2 - x \,, \end{cases} \tag{1}$$

discovered by Malasoma [12]. This system is equivariant under an inversion symmetry, that is, it obeys to

$$\boldsymbol{f}(\Gamma \cdot \boldsymbol{x}) = \Gamma \cdot \boldsymbol{f}(\boldsymbol{x}) \tag{2}$$

where $\boldsymbol{x} \in \mathbb{R}^3(x, y, z)$ is the state vector and

$$\Gamma = \begin{bmatrix} -1 & 0 & 0 \\ 0 & -1 & 0 \\ 0 & 0 & -1 \end{bmatrix} \tag{3}$$

defines the inversion symmetry. While we previously focused on the two asymmetric attractors which are co-existing before the merging attractor crisis, we will now investigate the unique symmetric attractor remaining in the state space once the two asymmetric ones merged. All these attractors are bounded by a genus-one torus. The main difference between these two types of attractors is that the asymmetric ones have a single folding while the symmetric attractor has two foldings [14]. This feature induces deep differences in their topological analysis. Let us start by summarizing the results we obtained for the two asymmetric attractors $\mathcal{A}$ and $\overline{\mathcal{A}}$ as discussed in [3]; this will help us to introduce some conventions and concepts we need for the analysis of the symmetric attractor $\mathcal{A}_s$. The bar will be used for designating the image object $\overline{O}$ obtained from an object O under the inversion symmetry.

In our previous paper [3], we introduced a convention to represent the attractor with a clockwise flow. In order to uniquely orientate the first-return map, we also proposed to work with cylindrical coordinates (r, θ, z) to investigate these attractors:

the range for values of radius r_n at the nth intersection with the Poincaré section S_i was normalized to the unit interval $]0,1[$, and oriented from the inner part (0) of the attractor to its periphery (1). The normalized variable is designated by $\rho_{i,n}$. Four equivalent Poincaré sections were useful for describing accurately the different elements of the two co-existing asymmetric attractors $\mathcal{A}$ and $\overline{\mathcal{A}}$ [3]. These Poincaré sections S_i $(i \in \{a,b,c,d\})$ are defined as

$$\mathcal{P}_i \equiv \left\{ (r_n, z_n) \in \mathbb{R}^2 \mid \theta_n = \varphi_i, \dot{\theta}_n < 0 \right\} \tag{4}$$

where $\varphi_a = \pi$, $\varphi_b = \frac{4\pi}{5}$, $\varphi_c = 0$, and $\varphi_d = \frac{9\pi}{5}$. For $\alpha = 2.0645$, we designated by $\mathcal{A}$ the attractor solution to system (1) and issued from initial conditions $(x_0, y_0, z_0) = (4, 0, 0)$ and, by $\overline{\mathcal{A}}$ its symmetric — under the inversion symmetry — from initial conditions $(x_0, y_0, z_0) = (-4, 0, 0)$ (Figure 1).

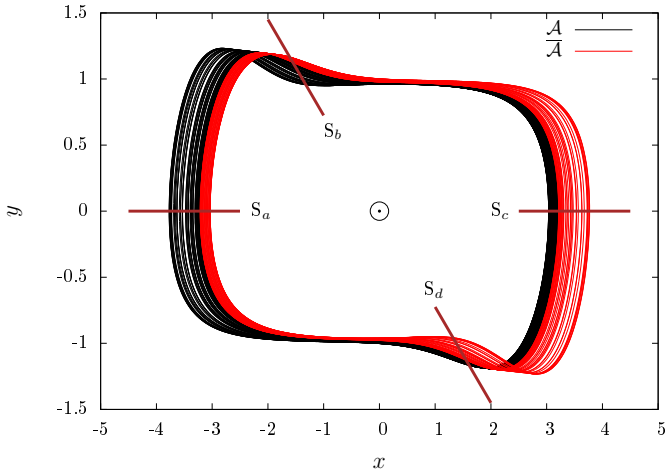

Figure 1. (Color online) Coexisting asymmetric attractors, $\mathcal{A}$ (black) and $\overline{\mathcal{A}}$ (red) solution to system (1) and issued from two symmetric sets of initial conditions. Parameter value $\alpha = 2.0645$.

2.2. Bifurcations diagram

In their analysis [14], Letellier and Malasoma provided two bifurcation diagrams, one for the original system and another for the image system, a system for which the inversion symmetry was modded out [21]. When computed from two symmetric sets of initial conditions $(x_0, y_0, z_0) = (4, 0, 0)$ and $(x_0, y_0, z_0) = (-4, 0, 0)$, the so-merged bifurcation diagrams (Figure 2) look similar to the diagram obtained from the image system as done in [14], but where the two asymmetric attractors can be distinguished.

For each of the two symmetric sets of initial conditions, the bifurcation diagram (Figure 2) exhibits a period-doubling cascade which is a common route to chaos. These diagrams also reveal that for $\alpha > 2.0644$ two asymmetric attractors coexist in the state space. After a merging attractor crisis at $\alpha < 2.0644$, the range of realized x_n-values in the Poincaré section does no longer depend on the initial conditions. This means that there is a unique symmetric attractor; in other words, the attractor is mapped into itself under the inversion symmetry. The two attractors $\mathcal{A}$ and $\overline{\mathcal{A}}$ co-existing in the state space for $\alpha = 2.0645$ (Figure 1) merged in a unique symmetric attractor $\mathcal{A}_s$ solution to system (4) when α is decreased.

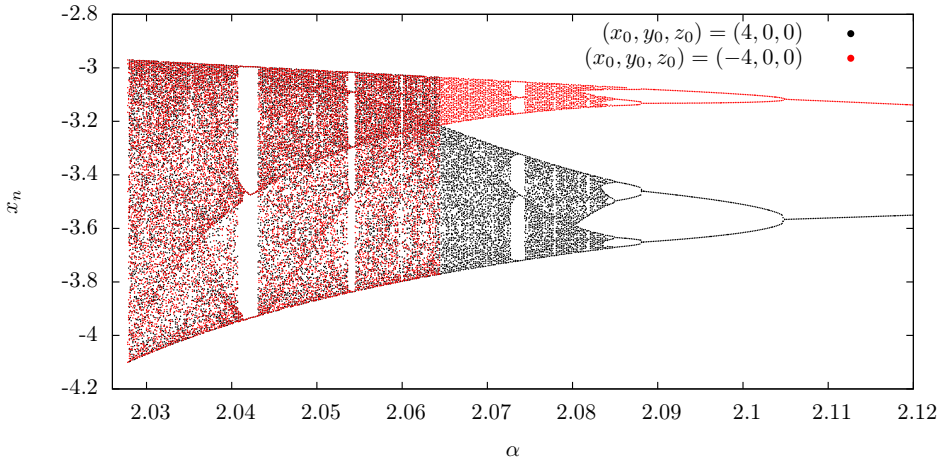

Figure 2. (Color online) Bifurcation diagram of system (1) computed in Poincaré section S_a versus parameter α and from two sets of initial conditions.

2.3. Templates and return maps

Attractor $\mathcal{A}$ ($\overline{\mathcal{A}}$) has a negative (positive) torsion τ_{-1} (τ_{+1}) between the two sections S_a and S_b (S_c and S_d) (Fig. 1). Torsion τ_{-1} (τ_{+1}) is a negative (positive) π-twist: consequently, τ_{-1} is mapped into τ_{+1} under the inversion symmetry. Direct templates $\mathcal{T}^1_{Dc}(\mathcal{A})$ and $\mathcal{T}^1_{Da}(\overline{\mathcal{A}})$ for these two attractors are shown in Figures 3a and 3b. As justified later in this paper, we designated by $\mathcal{T}^n_D$ the direct template of an attractor using a n-component Poincaré section. Subscript a (c) indicates the considered section and its corresponding branch line. In the present case, a single-component Poincaré section is used and, consequently, the template is designated by $\mathcal{T}^1_{Da}$ when the branch line associated with section S_a is considered. The template for attractor $\mathcal{A}$ can be obtained from the template for attractor $\overline{\mathcal{A}}$ (Fig. 3b) by applying the inversion symmetry and adding a permutation between the branches of the template $\mathcal{T}^1_{Dc}(\mathcal{A})$ so obtained (shown after the Poincaré section S_b in Figure 3a) to those of template $\mathcal{T}^1_{Da}(\overline{\mathcal{A}})$ to match with the standard insertion convention (see [3], for details). These two templates are drawn together to sketch what happens at the merging attractor crisis (Figure 3c). In this representation, the inversion symmetry is yet explicit because mixer $\mathcal{M}^1_{Da}$ ($\mathcal{M}^1_{Dc}$) between section S_b and branch line l_c (S_c and branch line l_a) is symmetric of the other. Indeed, $\mathcal{M}^1_{Dc}$ is the image of mixer $\mathcal{M}^1_{Da}$ under the inversion symmetry since $\mathcal{M}^1_{Dc} = \overline{\mathcal{M}}^1_{Da}$ and their linking matrices are such as

$$L^1_{Da}(\overline{\mathcal{A}}) = \overline{L}^1_{Dc}(\mathcal{A}) = \overline{\left[\!\left[\begin{array}{cc} -1 & -1 \\ -1 & 0 \end{array} \right]\!\right]} = \left[\!\left[\begin{array}{cc} 1 & 0 \\ 0 & 0 \end{array} \right]\!\right]. \tag{5}$$

In this equation, the left bracket of the linking matrix means that there is a splitting chart (in the present case, located after section S_b as shown in Figure 3a and dividing the attractor in two branches) and the right double bracket means that there is a branch line at the end of this linker where the (two) branches are merged (by squeezing) to form a single branch. Figure 3c suggests how these two templates merged, leading to an attractor with two mixers, one being the symmetric of the other.

The first-return maps to Poincaré section S_a are computed before ($\alpha = 2.0645$) and after ($\alpha = 2.0643$) the merging attractor crisis (Figure 4). When two asymmetric

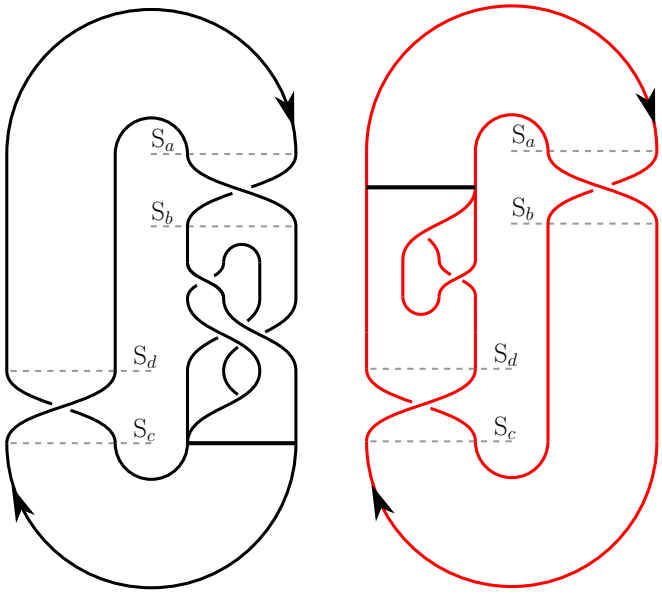

(a) Direct template $\mathcal{T}^1_{Dc}(\mathcal{A})$ (b) Direct template $\mathcal{T}^1_{Da}(\overline{\mathcal{A}})$

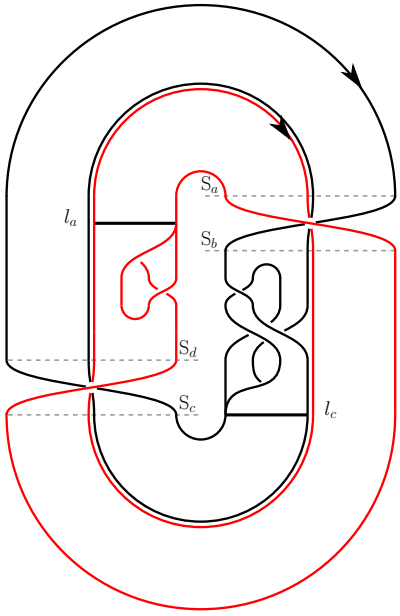

(c) The two direct templates $\mathcal{T}^1_{Dc}(\mathcal{A})$ and $\mathcal{T}^1_{Da}(\overline{\mathcal{A}})$

Figure 3. Direct templates for attractors $\mathcal{A}$ and $\overline{\mathcal{A}}$ and how they merged into a single one through the merging attractor crisis. Branch line l_c (l_a) can be associated with section S_c (S_a) since they are only separated by trivial branches.

attractors coexist, there are two disjoint unimodal first-return maps (Figure 4a). After the crisis, the two return maps merged into a single bimodal map (Figure 4b).

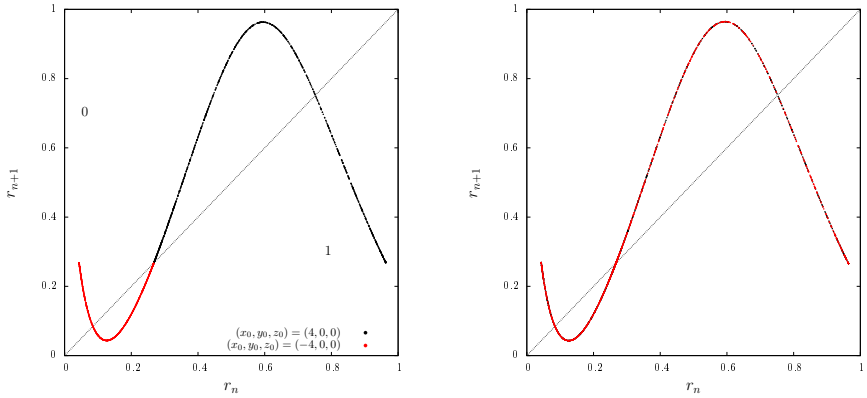

(a) Before the crisis: $\alpha = 2.0645$ (b) After the crisis: $\alpha = 2.027$

Figure 4. (Color online) First-return maps to Poincaré section S_a for the asymmetric attractors $\mathcal{A}$ and $\overline{\mathcal{A}}$ before the merging attractor crisis (a) and for the symmetric attractor $\mathcal{A}_s$ after the crisis (b).

3. Reduced template using a one-component Poincaré section

The symmetric attractor $\mathcal{A}_s$ solution to system (1) is investigated for $\alpha = 2.027$ (Figure 5). We introduced a symbolic dynamics in such a way that each symbol of the set $\Sigma_a^1(\mathcal{A}_s) = \{1, 2, 3, 4\}$ is associated with one of the branches of the first-return map as shown in Figure 6a. Parity of the symbols is related to the branch slope, that is, an odd (even) symbol is associated with an increasing (decreasing) branch [19]. In fact, the α-value is chosen in such a way that the first-return map has four branches and is associated with a complete symbolic dynamics, that is, with a situation for which each symbolic sequence encoded using the four symbols (one per branch) is actually realized. Such a complete trimodal map is directly the product of two complete unimodal smooth map as investigated in [13]. The attractor is bounded by a genus-one torus meaning that a one-component Poincaré section is sufficient to completely characterize the attractor (at least when the inversion symmetry is ignored).

Table 1. Linking numbers between pairs of unstable periodic orbits extracted from the symmetric chaotic attractor $\mathcal{A}_s$ solution to system (1). Parameter value: $\alpha = 2.027$.

	(1)	(2)	(3)	(23)	(12)
(2)	0				
(3)	0	0			
(23)	0	0	-1		
(12)	1	0	0	0	
(134)	1	0	-1	-1	1

Periodic orbits are numerically extracted from the first-return map and we computed linking numbers between pairs of orbits (Table 1). These linking numbers

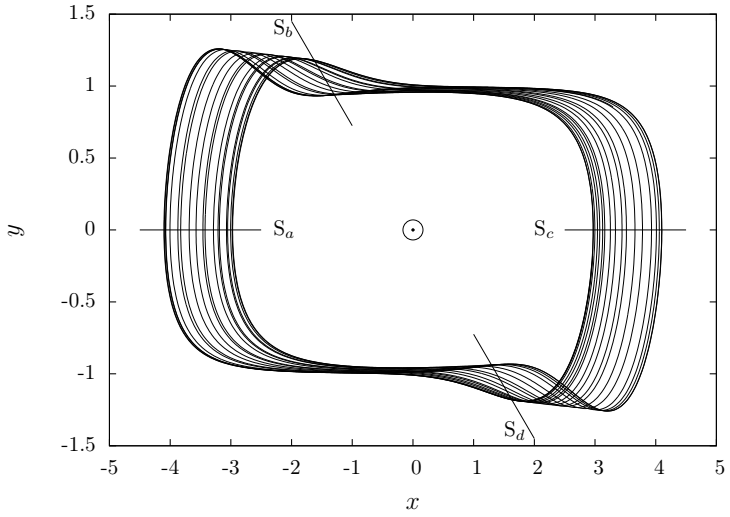

Figure 5. Symmetrical attractor $\mathcal{A}_s$ solution to system (1). Parameter value: $\alpha = 2.027$.

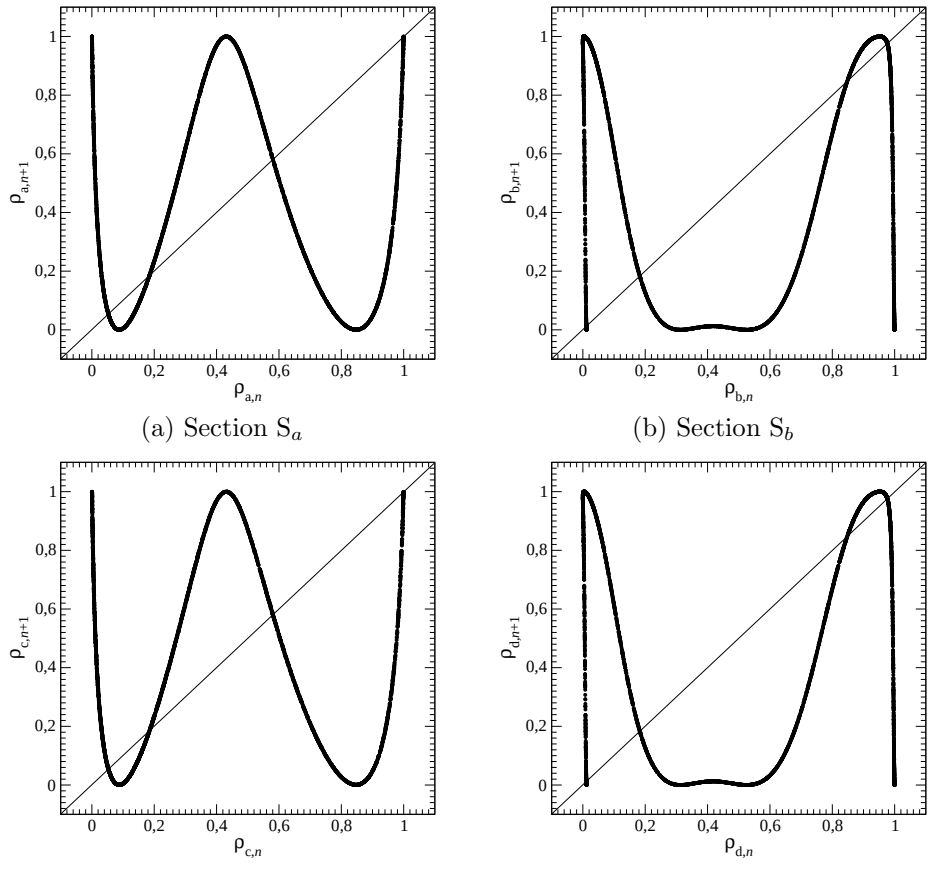

(a) Section S$_a$ (b) Section S$_b$

(c) Section S$_c$ (d) Section S$_d$

Figure 6. First-return maps to the one-component Poincaré section S$_i$ of the symmetrical attractor $\mathcal{A}_s$ solution to system (1). Parameter value: $\alpha = 2.027$.

can be recovered with the mixer $\mathcal{M}^1_{Ra}(\mathcal{A}_s)$ defined by the linking matrix

$$L^1_{Ra}(\mathcal{A}_s) = \begin{bmatrix} 1 & 0 & 0 & 0 \\ 0 & 0 & -1 & -1 \\ 0 & -1 & -1 & -1 \\ 0 & -1 & -1 & 0 \end{bmatrix}_a \tag{6}$$

describing the reduced template corresponding to branch line l_a (not distinguished from the Poincaré section S_a). The subscript a at the right double bracket designates the branch line (or equivalently in our approach the considered component of the Poincaré section) used to define the natural order over the symbols, that is, in the present case using $1 \lhd 2 \lhd 3 \lhd 4$. The template associated with mixer $\mathcal{M}^1_{Ra}(\mathcal{A}_s)$ is shown in Figure 7. Providing such a template for attractor $\mathcal{A}_s$ does not provide a topological description evidencing the symmetry properties of the attractor. In the next section, we will therefore investigate attractor $\mathcal{A}_s$ in order to evidence its symmetry properties.

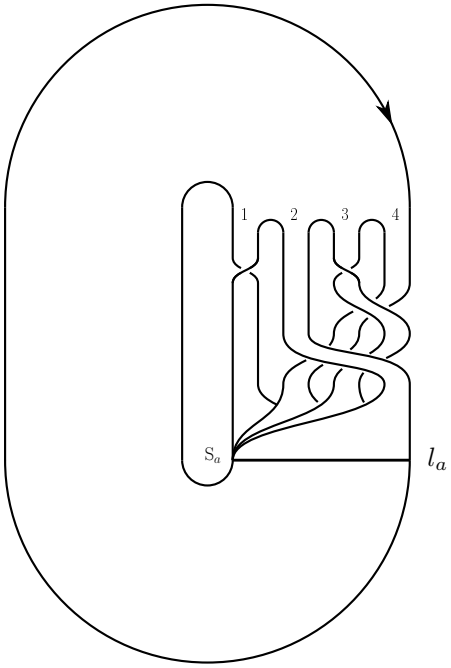

Figure 7. Reduced template $\mathcal{T}^1_{Ra}(\mathcal{A}_s)$ for the attractor $\mathcal{A}_s$ solution to the simplest equivariant jerk system. Parameter value $\alpha = 2.027$.

4. Templates using a two-component Poincaré section

Despite the fact that attractor $\mathcal{A}_s$ is bounded by a genus-one torus, it can be convenient to investigate such an attractor invariant under an order-2 symmetry (an inversion is an order-2 symmetry since $\Gamma^2 = I$ where I is the identity matrix) by using a two-component Poincaré section. The underlying idea is that such an attractor has two foldings whose squeezing mechanisms are located at branch lines l_a and l_c. Since branch lines l_a and Poincaré section S_a (l_c and S_c) are only separated by a trivial

branch, l_a and l_c can be identified to Poincaré sections S_a and S_c, respectively. A two-component Poincaré section $\mathcal{P}_2$ is thus defined as

$$\begin{aligned}\mathcal{P}_2 \equiv \mathrm{S}_a \cup \mathrm{S}_c = &\left\{(\rho_{a,n}, z_n) \in \mathbb{R}^2 \mid \theta_n = \varphi_a, \dot{\theta}_n < 0\right\} \cup \\ &\left\{(\rho_{c,n}, z_n) \in \mathbb{R}^2 \mid \theta_n = \varphi_c, \dot{\theta}_n < 0\right\}\end{aligned} \tag{7}$$

where $\rho_{a,n} \in]0,1[$ and $\rho_{c,n} \in]0,1[$ are the working variables in the unit interval for each branch line. They can be rewritten as a single variable

$$\rho_n = \mathbf{1}_{\mathrm{S}_a} \cdot \rho_{a,n} + \mathbf{1}_{\mathrm{S}_c} \cdot (1 + \rho_{c,n}) \tag{8}$$

where $\mathbf{1}_{\mathrm{S}_i}$ is the indicator function such as $\mathbf{1}_{\mathrm{S}_a} = 1$ when $\theta_n = \varphi_a$ and zero otherwise and $\mathbf{1}_{\mathrm{S}_c} = 1$ when $\theta_n = \varphi_c$, and zero otherwise.

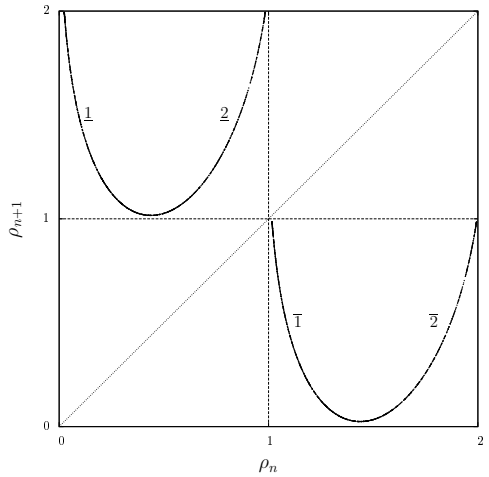

Figure 8. First-return map to the Poincaré section $\mathcal{P}_2$ of the symmetric attractor $\mathcal{A}_s$. There are two unimodal smooth maps, one being the symmetric of the other under the inversion symmetry. Parameter value: $\alpha = 2.027$.

The first-return map to the Poincaré section $\mathcal{P}_2$ (Figure 8) can be viewed as made of two unimodal smooth maps, one being the symmetric of the other under the inversion symmetry and the signature of each folding. Both are located in the off-diagonal panels of the first-return map to Poincaré section $\mathcal{P}_2$ (Figure 8), meaning that any point from S_a ($\rho_n \in]0;1[$) is sent to S_c ($\rho_n \in]1;2[$), thus leading to the transition matrix

$$\mathrm{Tr} = \begin{bmatrix} 0 & 1 \\ 1 & 0 \end{bmatrix} \tag{9}$$

between the components of the Poincaré section; the transition matrix is written using the order $\mathrm{S}_a \prec \mathrm{S}_c$. From the structure of the first-return map (Figure 8), it is possible to define a symbolic dynamics using four symbols, one for each monotonic branch. As commonly used [13, 14, 19, 22, 23], the parity of the symbol (an integer) is chosen according to the slope of the corresponding monotonic branch, that is, odd (even) for a branch with a negative (positive) slope. In order to explicit the symmetry, we will use symbol $\overline{\sigma}$ ($\underline{\sigma}$) for the S_a (S_c) component. We thus propose the set of symbols $\Sigma^2(\mathcal{A}_s) = \{\overline{1}, \overline{2}, \underline{1}, \underline{2}\}$, branch $\overline{1}$ ($\overline{2}$) being the symmetric companion to branch $\underline{1}$ ($\underline{2}$).

Periodic orbits are necessarily the same as those extracted from the single-component Poincaré section. Indeed, it is possible to map the orbital sequence assigned using a single-component Poincaré section (thus using the symbol set $\Sigma_a^1(\mathcal{A}_s)$ as in Section 3) into the orbital sequence associated with Poincaré section $\mathcal{P}_2$ (using the symbol set $\Sigma^2(\mathcal{A}_s)$) as it was done in [13, 14]. Such a map between symbols from set $\Sigma_a^1(\mathcal{A}_s)$ and those from set $\Sigma^2(\mathcal{A}_s)$ reads as

$$\Phi_a = \left| \begin{array}{l} \Phi_a(1) = \underline{1}\ \overline{2} \\ \Phi_a(2) = \underline{1}\ \overline{1} \\ \Phi_a(3) = \underline{2}\ \overline{1} \\ \Phi_a(4) = \underline{2}\ \overline{2}\,. \end{array} \right. \tag{10}$$

Few remarks must be done here. First, the fact that we switched from a single-component to a two-component Poincaré section induces that one symbol in the former Poincaré section is mapped into two symbols in the latter one. When a two-component Poincaré section is used, the topological period of an orbit, directly related to the number of symbols used to describe it, is therefore no longer associated with the number of revolutions made around the inner singular point but rather to the number of times it crosses the Poincaré section. The topological period of an orbit is thus directly related to the number of components used for defining the Poincaré section. Second, the parity of the symbols is preserved by map $\Phi_a : \Sigma_a^1(\mathcal{A}_s) \to \Sigma^2(\mathcal{A}_s)$ in the sense that the parity of a symbol σ^1 from $\Sigma_a^1(\mathcal{A}_s)$ is the same as the parity of the symbol sequence $\sigma_1^2\sigma_2^2$ from $\Sigma^2(\mathcal{A}_s)$ where $\Phi_a(\sigma^1) = \sigma_1^2\sigma_2^2$. For instance, symbol "1" designating a trajectory visiting branch 1 of the reduced template shown in Fig. 7 also corresponds to a trajectory that visits branch $\underline{1}$ of mixer $\mathcal{M}_c^2(\mathcal{A}_s)$ and then branch $\overline{2}$ of mixer $\mathcal{M}_a^2(\mathcal{A}_s)$: the odd symbol "1" is thus mapped into the odd sequence "$\underline{1}\overline{2}$".

In section 3, we constructed a template $\mathcal{T}_R^1(\mathcal{A}_s)$ using a single branch line (or equivalently a one-component Poincaré section) as shown in Figure 7. We thus obtained a branched manifold where the inversion symmetry was not explicit. When two branch lines are used, the construction of the branched manifold is somehow more natural as evidenced by the direct template $\mathcal{T}_D^2(\mathcal{A}_s)$ shown in Figure 9a. The two branch lines are designated by l_a and l_c, respectively; one branch line is the symmetric of the other under the inversion symmetry as in the symmetric attractor shown in Figure 5a. The two global torsions τ_{-1} and τ_{+1} are located between section S_a and S_b, and between S_c and S_d, respectively. In Figure 9a, the mixer occurring between S_b and l_c, is the symmetric of the mixer observed between S_d and l_a; the permutation between branches $\underline{1}$ and $\underline{2}$, which does not occur between branches $\overline{1}$ and $\overline{2}$, is only due to the standard insertion convention (see [3] for details). It is now possible to reduce template $\mathcal{T}_D^2(\mathcal{A}_s)$ by injecting each global torsion in the mixer which follows, thus leading to the reduced template $\mathcal{T}_R^2(\mathcal{A}_s)$ shown in Figure 9b. In this reduced template, the parity of local torsion in each branch is clearly associated with the parity of the symbol used to designate it. For instance, branch $\overline{2}$ presents a negative torsion by -2: this is an even branch, that is, an orientation preserving branch.

The direct template (Figure 9a) is made of four elements as follows. When the flow is followed from S_a to itself, we have one negative global torsion

$$\tau_{-1} = \left| \begin{array}{cc} -1 & -1 \\ -1 & -1 \end{array} \right|_b , \tag{11}$$

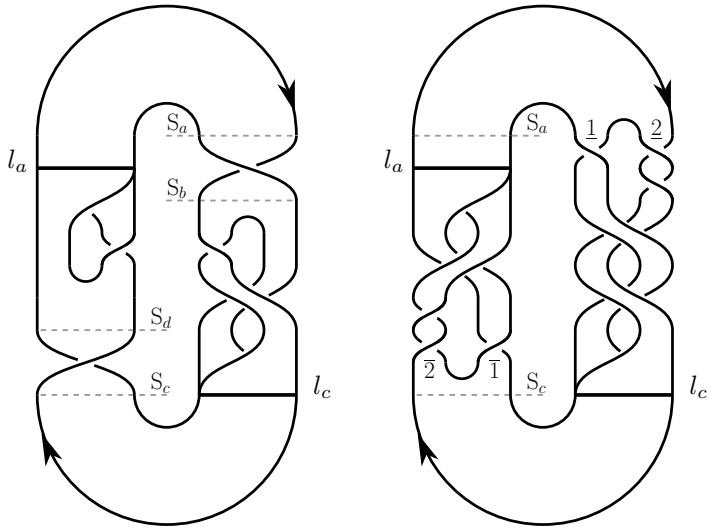

(a) Direct template $\mathcal{T}_R(\mathcal{A}_s)$ (b) Reduced template $\mathcal{T}_R^2(\mathcal{A}_s)$

Figure 9. Templates for the attractor shown in Figure 5a. Parameter value $\alpha = 0.027$.

one mixer

$$\mathcal{M}_{Dc}^2(\mathcal{A}_s) \equiv \left[\!\!\begin{array}{cc} -1 & -1 \\ -1 & 0 \end{array}\!\!\right]_c , \tag{12}$$

one positive global torsion

$$\tau_{+1} = \left| \begin{array}{cc} +1 & +1 \\ +1 & +1 \end{array} \right|_d , \tag{13}$$

and one mixer

$$\mathcal{M}_{Da}^2(\mathcal{A}_s) \equiv \left[\!\!\begin{array}{cc} +1 & 0 \\ 0 & 0 \end{array}\!\!\right]_a . \tag{14}$$

In [3], we showed that combining a linker $\mathcal{L}$ described by a linking matrix L with a global η-torsion $\mathcal{T}_\eta$ (expressed in η half-twists) leads to

$$\mathcal{L}' = \tau_\eta + \mathcal{L} \equiv \left| \begin{array}{ll} \tau_\eta + L & \text{if } \eta \text{ is even} \\ \tau_\eta + L^p & \text{if } \eta \text{ is odd} \end{array} \right. \tag{15}$$

where $\mathcal{L}'$ is the resulting linker and L^p is the permuted linking matrix whose elements L_{nm} are obtained from elements L_{mn} of matrix L [3]. Consequently, mixers $\mathcal{M}_{Da}^2(\mathcal{A}_s)$ and $\mathcal{M}_{Dc}^2(\mathcal{A}_s)$ can be algebraically reduced according to

$$\begin{aligned} &\mathcal{M}_{Rc}^2(\mathcal{A}_s) = \mathcal{T}_{-1} + \mathcal{M}_{Dc}^2(\mathcal{A}_s) \\ &\equiv \tau_{-1} + L_{Dc}^{2p}(\mathcal{A}_s) = \left| \begin{array}{cc} -1 & -1 \\ -1 & -1 \end{array} \right|_b + \left[\!\!\begin{array}{cc} -1 & -1 \\ -1 & 0 \end{array}\!\!\right]_c^p = \left[\!\!\begin{array}{cc} -1 & -2 \\ -2 & -2 \end{array}\!\!\right]_c = L_{Rc}^2(\mathcal{A}_s) \end{aligned} \tag{16}$$

and

$$\begin{aligned} &\mathcal{M}_{Ra}^2(\mathcal{A}_s) = \mathcal{T}_{+1} + \mathcal{M}_{Da}^2(\mathcal{A}_s) \\ &\equiv \tau_{-1} + L_{Da}^{2p}(\mathcal{A}_s) = \left| \begin{array}{cc} +1 & +1 \\ +1 & +1 \end{array} \right|_d + \left[\!\!\begin{array}{cc} +1 & 0 \\ 0 & 0 \end{array}\!\!\right]_a^p = \left[\!\!\begin{array}{cc} +1 & +1 \\ +1 & +2 \end{array}\!\!\right]_a = L_{Ra}^2(\mathcal{A}_s) , \end{aligned} \tag{17}$$

respectively. The reduced template $\mathcal{T}_R^2(\mathcal{A}_s)$ is thus made of the two mixers $\mathcal{M}_{Rc}^2(\mathcal{A}_s)$ and $\mathcal{M}_{Ra}^2(\mathcal{A}_s)$. Linking matrices L_{Ra}^2 and L_{Rc}^2 act from branches $\{\overline{1},\overline{2}\}$ to $\{\underline{1},\underline{2}\}$ and from branches $\{\underline{1},\underline{2}\}$ to branches $\{\overline{1},\overline{2}\}$, respectively.

5. Concatenation of mixers to obtain reduced templates

Our purpose is now to deduce the linking matrix $L_R^1(\mathcal{A}_s)$ of the unique mixer constituting the template when a one-component Poincaré section is used from the two linking matrices $L_{Ra}^2(\mathcal{A}_s)$ and $L_{Rc}^2(\mathcal{A}_s)$ corresponding to mixers $\mathcal{M}_{Ra}^2$ and $\mathcal{M}_{Rc}^2$ associated with branch lines l_a and l_c, respectively. When two mixers are concatenated, that is, one is applied after the other, the whole transformation corresponds to a product between the two linking matrices associated with the two mixers considered in the sense that the number of branches in the first mixer is multiplied by the number of branches in the second one. In the case of the symmetric attractor $\mathcal{A}_s$, there are two 2-branch mixers which are concatenated, namely mixers $\mathcal{M}_a^2$ and $\mathcal{M}_c^2$; the four-branch resulting mixer is, for instance, mixer $\mathcal{M}_c(\mathcal{A}_s)$ that we obtained in Eq. (6).

Let us introduce the set of symbols $\Sigma_i^1(\mathcal{A}_s)$ associated with each one-component Poincaré section S_i ($i \in \{a,b,c,d\}$) we already used for describing attractor $\mathcal{A}_s$. As shown in Figures 6, the orientation of the first-return map depends on the chosen Poincaré section S_i; such a feature reveals the presence of the two odd global torsions $\tau_{\pm 1}$ in the attractor. As already mentioned, the parity of symbols is related to the sign of branch slope. We can thus define four maps Φ_i transforming the symbols of set $\Sigma_a^2(\mathcal{A}_s)$ and $\Sigma_c^2(\mathcal{A}_s)$ into the symbols of set $\Sigma_i^1(\mathcal{A}_s)$ according to

$$\Phi_a = \begin{vmatrix} \Phi(1_a) = \underline{1}\ \overline{2} \\ \Phi(2_a) = \underline{1}\ \overline{1} \\ \Phi(3_a) = \underline{2}\ \overline{1} \\ \Phi(4_a) = \underline{2}\ \overline{2} \end{vmatrix}, \Phi_b = \begin{vmatrix} \Phi(0_b) = \underline{2}\ \overline{2} \\ \Phi(1_b) = \underline{2}\ \overline{1} \\ \Phi(2_b) = \underline{1}\ \overline{1} \\ \Phi(3_b) = \underline{1}\ \overline{2} \end{vmatrix}, \Phi_c = \begin{vmatrix} \Phi(1_c) = \overline{1}\ \underline{2} \\ \Phi(2_c) = \overline{1}\ \underline{1} \\ \Phi(3_c) = \overline{2}\ \underline{1} \\ \Phi(4_c) = \overline{2}\ \underline{2} \end{vmatrix}, \Phi_d = \begin{vmatrix} \Phi(0_d) = \overline{2}\ \underline{2} \\ \Phi(1_d) = \overline{2}\ \underline{1} \\ \Phi(2_d) = \overline{1}\ \underline{1} \\ \Phi(3_d) = \overline{1}\ \underline{2} \end{vmatrix}. \quad (18)$$

Symbols $\overline{\sigma}$ and $\underline{\sigma}$ designate which branches of mixers $\mathcal{M}_c^1(\mathcal{A}_s)$ and $\mathcal{M}_a^1(\mathcal{A}_s)$ are visited, respectively. In each pair of symbols, the first (second) one designates the branch of the first (second) mixer which is visited by the flow starting from a given Poincaré section S_i. When it will be necessary, we will add a subscript $i \in \{a,b,c,d\}$ to the symbols from sets $\Sigma_i^1(\mathcal{A}_s)$ to clearly specify to which Poincaré section S_i they refer to. Symbols from $\Sigma_i^1(\mathcal{A}_s)$ are chosen according to the natural order observed in the Poincaré section S_i constructed using variable $\rho_{i,n}$. The linking matrix $L_a^1(\mathcal{A}_s)$ is written according to the natural order of $\Sigma_i^1(\mathcal{A}_s)$.

We have thus to transform our multiplicative law between linking matrices

$$L_a^1(\mathcal{A}_s) = L_{Rc}^2(\mathcal{A}_s) \otimes L_{Ra}^2(\mathcal{A}_s) \quad (19)$$

into a sum of linking matrices. The composition law $\otimes$ is multiplicative in the sense that the dimension d_r of the matrix resulting from the concatenation of two others is the product of the dimension of the first by the dimension d_2 of the second. Nevertheless, the resulting matrix is obtained by summing $d_r \times d_r$ matrices. The 2×2 matrices L_{Rc}^2 and L_{Ra}^2 must therefore be "expanded" into 4×4 matrices. The first one occurring in the product $\otimes$ is expanded by transforming each element l_{mn} into a

2×2 block

$$\begin{matrix} l_{mn} & l_{mn} \\ l_{mn} & l_{mn} \end{matrix} . \tag{20}$$

Matrix $L^2_{Rc}(\mathcal{A}_s)$ is thus expanded into

$$L^1_{Rc}(\mathcal{A}_s) = \left| \begin{matrix} -1 & -1 & -2 & -2 \\ -1 & -1 & -2 & -2 \\ -2 & -2 & -2 & -2 \\ -2 & -2 & -2 & -2 \end{matrix} \right|_c \tag{21}$$

working between the natural order $1_a \lhd 2_a \lhd 3_a \lhd 4_a$ ($\underline{1\overline{2}} \lhd \underline{1\overline{1}} \lhd \underline{2\overline{1}} \lhd \underline{2\overline{2}}$) in section S_a and the natural order $1_c \lhd 2_c \lhd 3_c \lhd 4_c$ ($\overline{1}\underline{2} \lhd \overline{1}\underline{1} \lhd \overline{2}\underline{1} \lhd \overline{2}\underline{2}$) in Section S_c.

The second linking matrix is expanded from a $d_1 \times d_1$ matrix in which each element L_{ij} is replaced by a block B corresponding to the second linking matrix transformed as

$$L_{ij} = \left| \begin{matrix} B & L^2_{Rc,ii} \text{ and } L^2_{Rc,jj} \text{ are both even;} \\ B^{\text{-}} & L^2_{Rc,ii} \text{ is odd and } L^2_{Rc,jj} \text{ is even;} \\ B^{|} & L^2_{Rc,ii} \text{ is even and } L^2_{Rc,jj} \text{ is odd;} \\ B^p & L^2_{Rc,ii} \text{ and } L^2_{Rc,jj} \text{ are both odd.} \end{matrix} \right. \tag{22}$$

where

- $B^{\text{-}}$ is matrix B whose row order is reversed;
- $B^{|}$ is matrix B whose column order is reversed;
- B^p is matrix B which was permuted.

In the present case, the linking matrix $L^2_{Ra}(\mathcal{A}_s)$ is thus expanded as

$$L^1_{Ra}(\mathcal{A}_s) = \left| \begin{matrix} L^{2\,p}_{Ra} & L^{2}_{\overline{Ra}} \\ L^{2\,|}_{Ra} & L^{2}_{Ra} \end{matrix} \right|_a = \left| \begin{matrix} 2 & 1 & 1 & 2 \\ 1 & 1 & 1 & 1 \\ 1 & 1 & 1 & 1 \\ 2 & 1 & 1 & 2 \end{matrix} \right|_a \tag{23}$$

working between the natural order $1_c \lhd 2_c \lhd 3_c \lhd 4_c$ ($\overline{1}\underline{2} \lhd \overline{1}\underline{1} \lhd \overline{2}\underline{1} \lhd \overline{2}\underline{2}$) in the Poincaré section S_c and the natural order $1_a \lhd 2_a \lhd 3_a \lhd 4_a$ ($\underline{1\overline{2}} \lhd \underline{1\overline{1}} \lhd \underline{2\overline{1}} \lhd \underline{2\overline{2}}$) in section S_a.

In order to sum these two expanded matrices, it is necessary to check whether the four branches are well ordered at the output of the first mixer to be injected in the second mixer. This can be achieved by constructing a braid as follows. The symbolic sequences used for describing each branch are those used in the initial section, that is, in the present case, used in S_a. The upper line is the natural order of symbols in the initial Poincaré section, that is, in section S_a. Then the first expanded linking matrix is used to construct the first part of the braid (only permutation between branches are drawn, local torsions are omitted). In the example investigated, one can remark that, at the end of the first mixer (branch line l_c corresponding to the second row of symbol sequence in the braid shown in Figure 10a), the second branch, namely branch $\underline{1}\overline{2}$ should be sent to branch $\overline{2}$ of mixer $\mathcal{M}^2_{Ra}$ (since the second symbol is $\overline{2}$) while the third, namely branch $\underline{2}\overline{1}$, should be sent to branch $\overline{1}$ (the second symbol being $\overline{1}$). By definition, the left two branches issued of $\mathcal{M}^2_{Rc}$ are actually

sent to branch $\overline{1}$ of branch $\mathcal{M}^2_{Ra}$ while the right two branches are sent to branch $\overline{2}$. We thus have to insert a positive permutation between branch $\underline{1}\overline{2}$ and $\underline{2}\overline{1}$, that is, between the first and the third branches, to have the two branches $\underline{1}\overline{1}$ and $\underline{2}\overline{1}$ issued from $\mathcal{M}^2_{Rc}$ sent to branch $\overline{2}$, as their symbolic sequences suggest. In order to sum the expanded matrices describing the two mixers, additional permutations between branches is therefore required. Consequently, the 4×4 matrix

$$L^2_{\text{concat}} = \left| \begin{array}{cccc} 0 & 0 & 1 & 0 \\ 0 & 0 & 0 & 0 \\ 1 & 0 & 0 & 0 \\ 0 & 0 & 0 & 0 \end{array} \right|_c \tag{24}$$

must be added.

We have now the three linking matrices required to construct the linking matrix $L^1_a(\mathcal{A}_s)$ of mixer $\mathcal{M}^1_a(\mathcal{A}_s)$. We have

$$\begin{aligned} L^1_a(\mathcal{A}_s) &= L^2_{Rc} \otimes L^2_{Ra} \\ &= \left[\!\!\left[\begin{array}{cc} -1 & -2 \\ -2 & -2 \end{array} \right]\!\!\right]_c \otimes \left[\!\!\left[\begin{array}{cc} +1 & +1 \\ +1 & +2 \end{array} \right]\!\!\right]_a \\ &= \left[\!\!\left[\begin{array}{cccc} -1 & -1 & -2 & -2 \\ -1 & -1 & -2 & -2 \\ -2 & -2 & -2 & -2 \\ -2 & -2 & -2 & -2 \end{array} \right|_c + \left| \begin{array}{cccc} 0 & 0 & 1 & 0 \\ 0 & 0 & 0 & 0 \\ 1 & 0 & 0 & 0 \\ 0 & 0 & 0 & 0 \end{array} \right|_c + \left| \begin{array}{cccc} 2 & 1 & 1 & 2 \\ 1 & 1 & 1 & 1 \\ 1 & 1 & 1 & 1 \\ 2 & 1 & 1 & 2 \end{array} \right]\!\!\right]_a \\ &= \left[\!\!\left[\begin{array}{cccc} +1 & 0 & 0 & 0 \\ 0 & 0 & -1 & -1 \\ 0 & -1 & -1 & -1 \\ 0 & -1 & -1 & 0 \end{array} \right]\!\!\right]_a , \end{aligned} \tag{25}$$

from which the reduced braid can be easily drawn as shown in Fig. 10b.

Using branch line l_b as a reference, the mechanisms observed in the symmetric attractor are mixer $\mathcal{M}^2_c$, torsion $\mathcal{T}_{+1}$, mixer $\mathcal{M}^2_a$, torsion $\mathcal{T}_{-1}$, respectively. In that branch line, the natural order is

$$\underline{2}\overline{2} \lhd \underline{2}\overline{1} \lhd \underline{1}\overline{1} \lhd \underline{1}\overline{2} . \tag{26}$$

Before applying the product we have to reduce the three linking matrices τ_{-1}, $L^2_a(\mathcal{A}s)$ and τ_{+1} into a single one. The first step could be, for instance, to combine torsion $\mathcal{T}_{+1}$ with mixer $\mathcal{M}^2_a(\mathcal{A}_s)$ according to rule (15). We thus obtain

$$L^2_{Ra} = \left[\!\!\left[\begin{array}{cc} +1 & +1 \\ +1 & +2 \end{array} \right]\!\!\right]_a . \tag{27}$$

We can now combine this reduced mixer with torsion $\mathcal{T}_{-1}$. Since when the torsion is after the insertion branch of the mixer, there is no need for a permutation, we have thus

$$\mathcal{L}' = \mathcal{L} + \mathcal{T}_\eta \equiv L + \tau_\eta \quad (\forall \eta) . \tag{28}$$

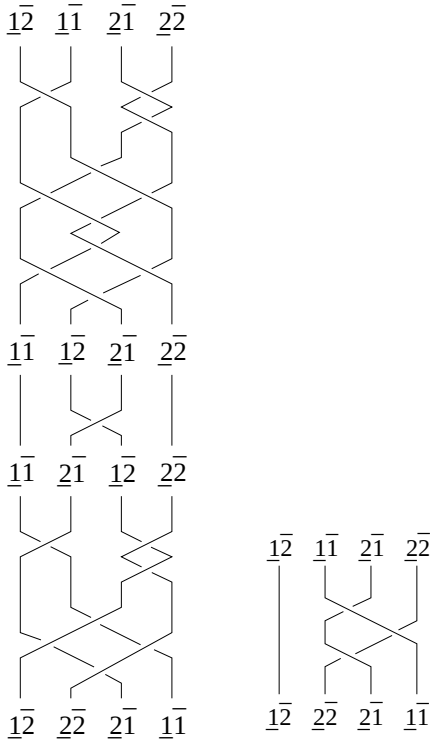

(a) Direct braid (b) Reduced braid

Figure 10. Braids used for constructing the concatenation of the two mixers observed in the symmetric attractor $\mathcal{A}_s$. The topology is described with respect to branch line l_a.

The addition law between linking matrix and torsion is therefore not commutative. Mixer $\mathcal{L}^2_a(\mathcal{A}_s)$ is now expressed with respect to branch line l_b and thus becomes $\mathcal{L}^2_{Rb}(\mathcal{A}_s)$ whose linking matrix is

$$L^2_{Rb} = \left[\begin{array}{cc} 0 & 0 \\ 0 & +1 \end{array}\right]_b . \tag{29}$$

Adding an odd global torsion after a branch line does not require to permute the linking matrix of the mixer. We have thus

$$\begin{aligned} \mathcal{M}^2_{Rb}(\mathcal{A}_s) &= \mathcal{M}^2_{Dc} \otimes \mathcal{M}^2_{Rb} \\ &\equiv L^2_{Dc} \otimes L^2_{Rb} \\ &= \left[\begin{array}{cc} -1 & -1 \\ -1 & 0 \end{array}\right]_c \otimes \left[\begin{array}{cc} 0 & 0 \\ 0 & +1 \end{array}\right]_b . \end{aligned} \tag{30}$$

From the first part of the direct braid (Figure 11a), we observe that a permutation must be inserted between branch $\underline{1}\overline{2}$ and $\underline{2}\overline{1}$ (the second and the fourth with respect

to branch line l_b), leading to the matrix

$$L^2_{\text{concat}} = \left| \begin{array}{cccc} 0 & 0 & 0 & 0 \\ 0 & 0 & 0 & 1 \\ 0 & 0 & 0 & 0 \\ 0 & 1 & 0 & 0 \end{array} \right|_c . \tag{31}$$

The first linking matrix $L^2_{Dc}(\mathcal{A}_s)$ is expanded by transforming each element l_{mn} into a 2×2 block

$$\begin{array}{cc} l_{mn} & l_{mn} \\ l_{mn} & l_{mn} \end{array} \tag{32}$$

and the second linking matrix $L^2_{Rb}(\mathcal{A}_s)$ is expanded by using the transformation (22), leading to

$$L^1_{Rb}(\mathcal{A}_s) = \left| \begin{array}{cc} L^{2\,p}_{Rb} & L^{2\,-}_{Rb} \\ L^{2\,|}_{Rb} & L^2_{Rb} \end{array} \right|_b = \left| \begin{array}{cccc} +1 & 0 & 0 & +1 \\ 0 & 0 & 0 & 0 \\ 0 & 0 & 0 & 0 \\ +1 & 0 & 0 & +1 \end{array} \right|_b . \tag{33}$$

We thus obtain the linking matrix of the reduced mixer

$$\begin{aligned} L^1_{Rb}(\mathcal{A}_s) &= L^2_{Dc} \otimes L^2_{Rb} \\ &= \left[\!\!\left[\begin{array}{cc} -1 & -1 \\ -1 & 0 \end{array} \right]\!\!\right]_c \otimes \left[\!\!\left[\begin{array}{cc} 0 & 0 \\ 0 & +1 \end{array} \right]\!\!\right]_b \\ &= \left[\!\!\left[\left| \begin{array}{cccc} -1 & -1 & -1 & -1 \\ -1 & -1 & -1 & -1 \\ -1 & -1 & 0 & 0 \\ -1 & -1 & 0 & 0 \end{array} \right|_c + \left| \begin{array}{cccc} 0 & 0 & 0 & 0 \\ 0 & 0 & 0 & 1 \\ 0 & 0 & 0 & 0 \\ 0 & 1 & 0 & 0 \end{array} \right|_c + \left| \begin{array}{cccc} 1 & 0 & 0 & 1 \\ 0 & 0 & 0 & 0 \\ 0 & 0 & 0 & 0 \\ 1 & 0 & 0 & 1 \end{array} \right|_b \right]\!\!\right]_b \\ &= \left[\!\!\left[\begin{array}{cccc} 0 & -1 & -1 & 0 \\ -1 & -1 & -1 & 0 \\ -1 & -1 & 0 & 0 \\ 0 & 0 & 0 & +1 \end{array} \right]\!\!\right]_b . \end{aligned} \tag{34}$$

This matrix is in fact the permuted matrix $L^{1p}_a(\mathcal{A}_s)$, a permutation induced by the torsion $\mathcal{T}_{-1}$ which is present between sections S_a and S_b.

Let us now treat the case of linking matrix $M_{Rc}(\mathcal{A}_s)$. From branch line l_c to itself, we have the mechanisms, $\mathcal{T}_{+1}$, $\mathcal{M}^2_a$, $\mathcal{T}_{-1}$, and $\mathcal{M}^2_c$. The best way is to combine each torsion with the next mixer, that is, to construct

$$\mathcal{M}^2_{Ra} = \mathcal{T}_{+1} \oplus \mathcal{M}^2_{Da} \tag{35}$$

and

$$\mathcal{M}^2_{Rc} = \mathcal{T}_{-1} \oplus \mathcal{M}^2_{Dc} . \tag{36}$$

We have thus

$$L^2_{Ra} = \left| \begin{array}{cc} +1 & +1 \\ +1 & +1 \end{array} \right| + \left[\!\!\left[\begin{array}{cc} +0 & +0 \\ +0 & +1 \end{array} \right]\!\!\right] = \left[\!\!\left[\begin{array}{cc} +1 & +1 \\ +1 & +2 \end{array} \right]\!\!\right] \tag{37}$$

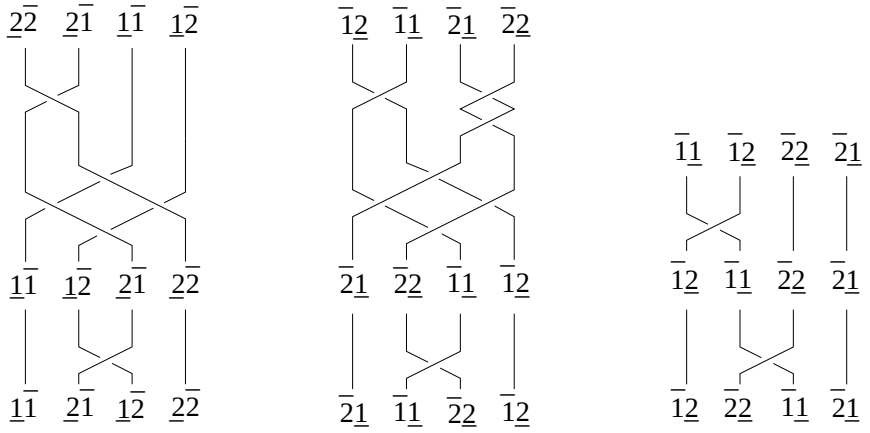

(a) From branch line l_b (b) From branch line l_c (c) From branch line l_d

Figure 11. First part of the braids corresponding to the relative organization of the branches within the symmetric attractor $\mathcal{A}_s$ and starting from different branch lines.

and

$$L^2_{Rc} = \left| \begin{array}{cc} -1 & -1 \\ -1 & -1 \end{array} \right| + \left[\!\!\left[\begin{array}{cc} 0 & -1 \\ -1 & -1 \end{array} \right]\!\!\right] = \left[\!\!\left[\begin{array}{cc} -1 & -2 \\ -2 & -2 \end{array} \right]\!\!\right]. \tag{38}$$

Between these two matrices, an additional permutation $\overline{1}\underline{1}$ and $\overline{2}\underline{2}$, that is, between the second and the fourth branches, is required as revealed by the direct braid shown in Figure 11b. The linking matrix $L^1_{Ra}(\mathcal{A}_s)$ must be expanded in the trivial way and matrix L^1_{Rc} must be expanded according to transformation (22), that is, according to

$$\left| \begin{array}{cc} L^{2p}_{Rc} & L^{2--}_{Rc} \\ L^{2|}_{Rc} & L^{2}_{Rc} \end{array} \right|_c . \tag{39}$$

We thus have

$$\begin{aligned} L^1_{Rc}(\mathcal{A}_s) &= L^2_{Ra} \otimes L^2_{Rc} \\ &= \left[\!\!\left[\begin{array}{cc} +1 & +1 \\ +1 & +2 \end{array} \right]\!\!\right]_a \otimes \left[\!\!\left[\begin{array}{cc} -1 & -2 \\ -2 & -2 \end{array} \right]\!\!\right]_c \\ &= \left[\!\!\left[\begin{array}{cccc} 1 & 1 & 1 & 1 \\ 1 & 1 & 1 & 1 \\ 1 & 1 & 2 & 2 \\ 1 & 1 & 2 & 2 \end{array} \right]\!\!\right|_c + \left| \begin{array}{cccc} 0 & 0 & 0 & 0 \\ 0 & 0 & 0 & 1 \\ 0 & 0 & 0 & 0 \\ 0 & 1 & 0 & 0 \end{array} \right|_c + \left|\!\!\left[\begin{array}{cccc} -2 & -2 & -2 & -2 \\ -2 & -1 & -1 & -2 \\ -2 & -1 & -1 & -2 \\ -2 & -2 & -2 & -2 \end{array} \right]\!\!\right]_c \\ &= \left[\!\!\left[\begin{array}{cccc} -1 & -1 & -1 & -1 \\ -1 & 0 & 0 & 0 \\ -1 & 0 & +1 & 0 \\ -1 & 0 & 0 & 0 \end{array} \right]\!\!\right]_c . \end{aligned} \tag{40}$$

Matrix $L^1_{Rc}(\mathcal{A}_s)$ is the symmetric of matrix $L^1_{Ra}(\mathcal{A}_s)$, that is, it obeys to

$$L^1_{Rc}(\mathcal{A}_s) = -L^1_{Ra}(\mathcal{A}_s) - \begin{vmatrix} 0 & +1 & +1 & +1 \\ +1 & 0 & +1 & +1 \\ +1 & +1 & 0 & +1 \\ +1 & +1 & +1 & 0 \end{vmatrix} = \overline{L}^1_{Ra}(\mathcal{A}_s) \tag{41}$$

as it was established in [3].

The last case to treat is when the template starts from branch line l_d. As we did for the case of mixer $\mathcal{M}^1_b(\mathcal{A}_s)$, we can reduced the linking matrices corresponding to torsion $\mathcal{T}_{-1}$, mixer $\mathcal{M}^2_{Da}(\mathcal{A}_s)$ and torsion $\mathcal{T}_{+1}$ into the single reduced matrix

$$\mathcal{L}^2_{Rd}(\mathcal{A}_s) = \left[\!\!\left[\begin{array}{cc} 0 & -1 \\ -1 & -1 \end{array} \right]\!\!\right]_d . \tag{42}$$

After expanding the linking matrices, we got

$$\begin{aligned} L^1_{Rd}(\mathcal{A}_s) &= L^2_{Da} \otimes L^2_{Rd} \\ &= \left[\!\!\left[\begin{array}{cc} +1 & 0 \\ 0 & 0 \end{array} \right]\!\!\right]_a \otimes \left[\!\!\left[\begin{array}{cc} 0 & -1 \\ -1 & -1 \end{array} \right]\!\!\right]_d \\ &= \left[\!\!\left[\begin{array}{cccc} +1 & +1 & 0 & 0 \\ +1 & +1 & 0 & 0 \\ 0 & 0 & 0 & 0 \\ 0 & 0 & 0 & 0 \end{array} \right]\!\!\right]_d + \left[\!\!\left[\begin{array}{cccc} 0 & 0 & 1 & 0 \\ 0 & 0 & 0 & 0 \\ 1 & 0 & 0 & 0 \\ 0 & 0 & 0 & 0 \end{array} \right]\!\!\right]_d + \left[\!\!\left[\begin{array}{cccc} -1 & -1 & -1 & -1 \\ -1 & 0 & 0 & -1 \\ -1 & 0 & 0 & -1 \\ -1 & -1 & -1 & -1 \end{array} \right]\!\!\right]_d \\ &= \left[\!\!\left[\begin{array}{cccc} 0 & 0 & 0 & -1 \\ 0 & +1 & 0 & -1 \\ 0 & 0 & 0 & -1 \\ -1 & -1 & -1 & -1 \end{array} \right]\!\!\right]_d . \end{aligned} \tag{43}$$

As shown in the braid issued from branch line l_d (Fig. 11c), it was necessary to permute branches $\overline{2}\underline{2}$ and $\overline{1}\underline{1}$ (first and third branches according to the natural order $\lhd_d$), and linking matrix $L^1_{Rd}(\mathcal{A}_s)$ was expanded according to transformation (22). Since there is only a torsion $\mathcal{T}_{+1}$ between mixers $\mathcal{M}^1_d(\mathcal{A}_s)$ and $\mathcal{M}^1_c(\mathcal{A}_s)$, we have

$$L^1_d(\mathcal{A}_s) = L^{1p}_c(\mathcal{A}_s) , \tag{44}$$

as expected. Moreover, mixer $\mathcal{M}^1_d(\mathcal{A}_s)$ is the symmetric of mixer $\mathcal{M}^1_b(\mathcal{A}_s)$, that is,

$$L^1_d(\mathcal{A}_s) = -L^1_b(\mathcal{A}_s) - \begin{vmatrix} 0 & +1 & +1 & +1 \\ +1 & 0 & +1 & +1 \\ +1 & +1 & 0 & +1 \\ +1 & +1 & +1 & 0 \end{vmatrix} = \overline{L}^1_b(\mathcal{A}_s) . \tag{45}$$

All these mixers are related according to

$$L^1_a(\mathcal{A}_s) = L^{1p}_b(\mathcal{A}_s) = \overline{L}^1_c(\mathcal{A}_s) = \overline{L}^{1p}_d(\mathcal{A}_s) . \tag{46}$$

These four mixers thus describe the same attractor $\mathcal{A}_s$.

6. Conclusion

Topological characterization is known to be a refined way to describe the mechanisms organizing unstable periodic orbits constituting the skeleton of chaotic attractors. In order to limit the number of possible templates for a given attractor, we introduced some conventions such as always representing the attractor with a clockwise flow and to compute first-return map with a variable normalized to the unit interval from the center to the periphery of the attractor. Nevertheless templates remain proposed using an arbitrarily chosen Poincaré section and, as we showed in this paper, many templates which look like different but are topologically equivalent can be obtained for a given attractor. Indeed, when there is a global torsion between two Poincaré sections, the resulting templates will be drawn in two different ways since branches are ordered in reversed ways. One template can be obtained from the other by permuting linking matrix.

In a companion paper, we showed that when mixers — associated with a branch line where branches are squeezed — are combined with open linker (without splitting chart nor branch line as global torsions are), the resulting mixer can be obtained using an additive law working on the linking matrices. In this paper we treated the case where two mixers are combined to form a single one (the so-called reduced mixer). In that case, a multiplicative law is required in the sense that the reduced mixer has a number of branches equal to the product of the number of branches in the first mixer by the number of branches in the second mixer. Rules for expanding linking matrices to the appropriate dimension were thus proposed to transform then the multiplicative law into an additive law. Manipulating algebraically linking matrices rather than drawing rather complex branched manifolds thus open new possibilities to construct templates of chaotic attractors characterized by first-return maps with a large number of branches and/or made of multiple mixers as often encountered in attractors produced by systems with large-order symmetry.

References

[1] T. D. Tsankov & R. Gilmore, Strange attractors are classified by bounding tori, *Physical Review letters*,**91** (13), 134104, 2003.
[2] R. Gilmore & M. Lefranc, *The topology of chaos*, Wiley, 2002.
[3] M. Rosalie & C. Letellier, Systematic template extraction from chaotic attractors. I-Genus-one attractors with an inversion symmetry, *Journal of Physics A*, **46**, 375101, 2013.
[4] O. E. Rössler, An equation for continuous chaos, *Physics Letters A*, **57** (5), 397-398, 1976.
[5] O. Decroly & A. Goldbeter, Birhythmicity, chaos and other patterns of temporal self-organization in a multiply regulated biochemical system, *Proceedings of the Natural Academy of Science* (USA), **79**, 6917-6921, 1982.
[6] J. C. Sprott, Some simple chaotic flows, *Physical Review E*, **50** (2), 647-650, 1994.
[7] R. K. Upadhyay, S. R. K. Jyengar & V. Rai, Chaos: an ecological reality?, *International Journal of Bifurcation & Chaos*, **8** (6), 1325-1333, 1998.
[8] B. Blasius, A. Huppert & L. Stone, Complex dynamics and phase synchronization in spatially extended ecological systems, *Nature*, **399**, 354i-359, 1999.
[9] C. Letellier & Aziz-Alaoui, Analysis of the dynamics of a realistic ecological model, *Chaos, Solitons & Fractals*, **13**, 95-107, 2002.
[10] C. Letellier & L. A. Aguirre, Required criteria for recognizing new types of chaos: application to the "Cord" attractor, *Physical Review E*, **85**, 036204, 2012.
[11] C. Letellier, F. Denis & L. A. Aguirre What can be learned from a chaotic cancer model?, *Journal of Mathematical Biology*, **322**, 7-16, 2013.
[12] J.-M. Malasoma, What is the simplest dissipative chaotic jerk equation which is parity invariant?, *Physics Letters A*, **264** (5), 383-389, 2000.

[13] C. Letellier, P. Dutertre, J. Reizner & G. Gouesbet, Evolution of a multimodal map induced by an equivariant vector field, *Journal of Physics A: Mathematical and General*, **29**, 5359-5373, 1996.

[14] C. Letellier & J.-M. Malasoma, Unimodal order in the image of the simplest equivariant chaotic system, *Physical Review E*, **64**, 067202, 2001.

[15] C. Grebogi, E. Ott & J. A. Yorke, Crises, sudden changes in chaotic attractors, and transient chaos, *Physica D*, **7**, 181-200, 1983.

[16] O. E. Rössler, Horseshoe map in the Lorenz equation, *Physical Letters A*, **60** (5), 392-394, 1977.

[17] N. B. Tufillaro, T. Abbott & J. Reilly, *An experimental approach to nonlinear dynamics and chaos*, Addison-Wesley, New York, 1992.

[18] R. Gilmore, Topological analysis of chaotic dynamical systems, *Reviews of Modern Physics*, **70** (4), 1455-1529, 1998.

[19] C. Letellier, P. Dutertre & B. Maheu, Unstable periodic orbits and templates of the Rössler system: toward a systematic topological characterization, *Chaos*, **5** (1), 271-282, 1995.

[20] G. B. Mindlin, X.-J. Hou, H. G. Solari, R. Gilmore & N. B. Tufillaro, Classification of strange attractors by integers, *Physical Review Letters*, **64**, 20, 1990.

[21] C. Letellier & G. Gouesbet, Topological characterization of reconstructed attractors modding out symmetries, *Journal de Physique II*, **6**, 1615-1638, 1996.

[22] L. Le Sceller, C. Letellier & G. Gouesbet, Algebraic evaluation of linking numbers of unstable periodic orbits in chaotic attractors, *Physical Review E*, **49** (5), 4693-4695, 1994.

[23] M. Rosalie & C. Letellier, Toward a general procedure for extracting templates from chaotic attractors bounded by high genus torus, *International Journal of Bifurcation and Chaos*, **24**(4), 1450045, 2014.